钩藤干预自发性高血压大鼠肝脏代谢紊乱的脂质组学研究

张世明[1], 齐冬梅[2], 曹艺明[1], 周洪雷[1], 蒋海强[2*], 李运伦[3], 张 倩[1]

(1. 山东中医药大学药学院, 山东 济南 250355; 2. 山东中医药大学实验中心, 山东 济南 250355;
3. 山东中医药大学附属医院, 山东 济南 250300)

摘要: 本文通过脂质组学方法研究钩藤干预自发性高血压大鼠肝脏脂质代谢物的变化, 探索钩藤的作用机制。所有实验过程均获得了山东中医药大学实验中心动物保护和使用委员会的批准。实验中采用UHPLC-Q Extractive轨道阱高分辨质谱采集大鼠肝脏脂质代谢物信息, 经模式识别, 识别显著差异的物质, 通过质谱和数据库检索鉴定潜在生物标志物。模式识别结果显示正常组与SHR组明显分开, 高血压大鼠与正常大鼠相比, 磷脂酰胆碱、甘油二酯、磷脂酸和鞘磷脂含量减少; 溶血磷脂酰胆碱、甘油三酯、亚油酸、花生四烯酸和鞘磷脂含量增多。钩藤乙醇提取物通过干预甘油磷脂代谢通路、鞘脂代谢通路、亚油酸代谢通路、花生四烯酸代谢通路改善脂质代谢紊乱的状态。本研究揭示了钩藤干预脂质代谢的机制, 在阐释中药作用方面显示出了独特的潜力。

关键词: 脂质组学; 肝脏; 自发性高血压大鼠; 钩藤; 高分辨质谱

中图分类号: R917 **文献标识码**: A **文章编号**: 0513-4870(2019)09-1636-09

Lipidomics study on intervention by *Uncaria* on hepatic metabolic disorder in spontaneously hypertensive rats

ZHANG Shi-ming[1], QI Dong-mei[2], CAO Yi-ming[1], ZHOU Hong-lei[1], JIANG Hai-qiang[2*], LI Yun-lun[3], ZHANG Qian[1]

(*1. School of Pharmacy, Shandong University of Traditional Chinese Medicine, Jinan 250355, China;*
2. Experiment Center of Shandong University of Traditional Chinese Medicine, Jinan 250355, China;
3. Affiliated Hospital of Shandong University of Traditional Chinese Medicine, Jinan 250300, China)

Abstract: In this paper, the lipidomics was used to analyze the changes to address how *Uncaria* interrupts lipid metabolism in the liver of spontaneously hypertensive rats, and to explore the mechanism of action of *Uncaria*. All the experiments were approved by the animal protection and use committee of Shandong University of Traditional Chinese Medicine. UHPLC-Q Extractive orbitrap high-resolution mass spectrometry was used to collect lipid metabolite information of the rat livers. Through pattern recognition, matters with noticeable differences were recognized. Mass spectrum and data base searching helped to identify the potential biomarkers. Pattern recognition results indicated that the rats from control *versus* SHR group showed clear differences. Compared with the rats from the control group, there are decreases in sphosphatidylcholine, phosphatidic acid, diacylglycerol and sphingomyelin in rats from the SHR group, however lysophosphatidylcholine, triglyceride, linoleic acid, arachidonic acid and ceramide are increased. *Uncaria* could regulate the disorder of lipid metabolism by interfering with glycerophospholipid, sphingolipid, linoleic acid, and arachidonic acid metabolic pathways. This study provided the mecha-

收稿日期: 2019-03-10; 修回日期: 2019-06-04.
基金项目: 国家自然科学基金资助项目 (81774173); 山东省博士基金资助项目 (ZR2016HB50); 山东省重大科技创新工程项目 (2017CXGC1307); 山东省重点研发计划资助项目 (2018GSF119007).
*通讯作者 Tel: 15966050664, E-mail: jhq12723@163.com
DOI: 10.16438/j.0513-4870.2019-0164

nistic understanding of the impact of *Uncaria* on lipid metabolism and revealed the lipid metabolism pathways affected to offer the explanation for the complex mechanism of action.

Key words: lipidomics; liver; spontaneous hypertensive rat; *Uncaria*; high resolution mass spectrometry

高血压是导致心血管疾病甚至死亡的主要因素之一[1], 是心血管疾病研究的重点[2]。脂质代谢紊乱是高血压病的主要易患因素[3]。近年来, 研究人员开始关注脂质代谢对高血压等心血管病的作用[4]。目前主要认为鞘磷脂、甘油磷脂类、甘油脂类、神经酰胺等脂质代谢物与高血压有密切关系[5-8]。

脂类代谢的主要器官和重要场所在肝脏[9]。甘油三酯 (triglyceride, TAG) 蓄积过多和游离脂肪酸 (free fatty acids, FFA)、总胆固醇、磷脂酰胆碱 (phosphatidylcholine, PC)、磷脂酰乙醇胺 (phosphatidyl ethanolamine, PE)、神经酰胺 (ceramide, Cer) 和鞘磷脂 (sphingolipid, SM) 异常的代谢是导致脂质代谢紊乱的主要原因[10-13], 而这些成分主要在肝脏细胞中产生和贮存[14,15]。脂质代谢紊乱是高血压的主要特征之一[3,16,17]。

脂质组学由 Han 和 Gross 在 2003 年提出[18]。脂质组学作为代谢组学的一个重要分支, 旨在表征脂质种类, 并研究脂质在生物系统中的代谢途径和网络。脂质组学用于发现和识别各种脂类物质结构, 研究体液和组织中脂质的分布, 以及研究脂质在不同生物种群之间的差异[19,20]。质谱法的广泛应用使得脂质组学分析更加精确和高效。脂质组学已经形成了一套成熟的分析方法, 并应用于生物医学科学中[21,22]。Graessler 等[16] 通过研究发现与正常血压男性相比, 男性高血压患者 PC-O (36∶4)、PC-O (38∶4)、PE-O (38∶5)、PE-O (38∶6) 和 PE-O (40∶5) 等甘油磷脂类成分降低。脂质组学分析发现高血压患者中磷脂类和甘油酯类代谢异常[23], 其中磷脂酰胆碱和甘油三酯是影响血脂代谢的主要因素[24]。

钩藤是治疗高血压和调节脂质代谢常用的天然药物, 能够预防脑血管硬化、降血压和降血脂[25,26]。钩藤中的钩藤碱具有镇静、抗惊厥及抗血小板聚集和血栓形成的药理作用[27]。钩藤碱抑制血管紧张素 II 诱导的大鼠血管平滑肌细胞增殖, 并进一步增加一氧化氮合酶活性, 促进一氧化氮合成和释放, 从而达到降血压的作用[28]。本文通过脂质组学方法, 研究钩藤对自发性高血压大鼠肝脏代谢絮乱的作用, 其中正常组和钩藤治疗组肝脏标志物相对含量的差异, 揭示了钩藤调节高血压大鼠脂质代谢紊乱的过程。本研究对钩藤治疗自发性高血压大鼠肝脏代谢絮乱的机制研究提供科学依据。

材料与方法

仪器和试剂 UltiMate 3000 超高效液相色谱仪 (美国 Thermo Fisher Scientific 公司), Q Exactive 四极杆-静电场轨道阱高分辨质谱仪 (美国 Thermo Fisher Scientific 公司), 配有 ESI 离子源。SCIENTZ-48 高通量组织研磨器 (宁波新芝生物科技股份有限公司), 高速台式离心机 (美国 Thermo Fisher Scientific 公司), Vortex-Genie 2 涡旋震荡器 (美国 SI 公司), BP-98A 大小鼠无创血压仪 (北京软隆技术有限公司), 20～200 μL 和 100～1 000 μL 单道微量可调移液器 (美国 Thermo Fisher Scientific 公司), 乙腈 (批号: 174263, Thermo Fisher 公司), 甲醇 (批号: 178511, Thermo Fisher 公司), 异丙醇 (批号: 178454, Thermo Fisher 公司), 甲基叔丁基醚 (批号: F1614018, methyl tert-butyl ether, MTBE) 购于上海阿拉丁生化科技股份有限公司), 甲酸铵 (批号: 20161008, 色谱纯, 上海迈坤化工有限公司), 钩藤药材 (原产地云南; 批号: 170906)。

药品制备 钩藤粉碎, 加 8 倍量 75% 乙醇浸泡 30 min, 回流提取 2 次, 每次 2 h, 合并 2 次提取液, 真空干燥, 4 ℃冰箱保存备用。采用 UHPLC-Q Exactive orbitrap MS 正离子模式定量分析钩藤生物碱, 最终测得以下 4 种指标成分相当于每克钩藤原药材中的含量为: 钩藤碱 (217.1 ± 1.7) μg、异钩藤碱 (126.7 ± 2.0) μg、去氢钩藤碱 (55.18 ± 0.67) μg、异去氢钩藤碱 (215.8 ± 2.5) μg。

实验动物 雄性自发性高血压大鼠 (spontaneously hypertension rats, SHR) 14 只, 清洁级, 8 周龄, 体重 (190.7 ± 9.0) g; 雄性 Wistar-Kyoto (WKY) 大鼠 7 只, 清洁级, 8 周龄, 体重 (155.3 ± 1.8) g。实验动物均购于北京维通利华实验动物技术有限公司, 合格证书: SCXK (京) 2016-0006。所有实验过程均获得了山东中医药大学实验中心动物保护和使用委员会的批准 (SDUTCM2018120301)。

动物分组 正常组 (7 只), SHR 模型组 (14 只)。正常喂养大鼠 7 天, 待大鼠适应环境、血压稳定后, 将 SHR 随机分为 2 组, 即: SHR 组 7 只, 钩藤组 7 只, 并选择 WKY 大鼠作为正常组。分笼饲养, 每笼各 7 只。饲养在 12 h 光照/黑暗的房间内, 室内温度为 23～25 ℃, 自由摄食进水。

动物给药与样品收集 钩藤组: 参照课题组前期

工作基础[3,29,30], 给药剂量为2.29 g·kg^{-1}体重钩藤乙醇提取物粉末。正常组和SHR组给予等量的生理盐水。每天定时给药, 每周给药6天, 连续给药4周。给药周期结束后, 所有大鼠禁食不禁水12 h后称重, 以10%水合氯醛对大鼠行腹腔麻醉 (3 mL·kg^{-1}), 待动物成功麻醉后 (用止血钳试探性的夹住大鼠的四肢, 大鼠无明显反应), 剪开腹腔, 取肝脏后, 用生理盐水清洗肝组织由深红变为浅红色。

样品前处理 脂质提取采用甲基叔丁基醚提取法[31]。取大鼠肝组织50 mg, 置于2 mL的离心管中, 加入甲醇水溶液 (1∶1) 1.2 mL, 高通量组织研磨器匀浆1 min。在4 °C下12 000 r·min^{-1}离心15 min。去除上清液向沉淀中加入甲基叔丁基醚−甲醇−水 (5∶1.5∶1.45) 1.6 mL, 涡旋5 min, 在4 °C下, 12 000 r·min^{-1}, 离心15 min, 上清液用氮气吹干。用1.2 mL异丙醇−乙腈−水的混合溶液 (2∶1∶1) 溶解。

色谱条件 色谱柱: Halo C_{18}柱 (100 mm×2.1 mm, 2.7 μm); 流速为0.30 mL·min^{-1}; 柱温45 ℃, 进样器温度15 ℃; 进样量2 μL。二元梯度系统包括5 mmol·L^{-1}醋酸铵加入乙腈−水的混合溶液 (40∶60; 流动相A) 和5 mmol·L^{-1}醋酸铵加入乙腈−异丙醇的混合溶液 (10∶90; 流动相B)。梯度为: 0～1 min流动相B比例为2%～20%; 1～5 min流动相B比例为20%～40%; 5～9 min流动相B比例为40%～70%; 9～17 min流动相B比例为70%～88%。

质谱检测模式 采用正负离子模式检测。正离子检测模式为: 离子源ESI; 毛细管电压3 500 V; 毛细管温度350 ℃; 鞘气45 arb; 辅助气10 arb; 源内温度320 ℃; 质谱采集范围*m*/*z* 300～1 300; 分辨率为70 000; S-Lens RF Level为55。负离子检测模式为: 离子源ESI; 毛细管电压3 000 V; 毛细管温度320 ℃; 鞘气45 arb; 辅助气10 arb; 源内温度300 ℃; 质谱采集范围*m*/*z* 300～1 300; 分辨率为70 000; S-Lens RF Level为55。正负离子二级质谱采集范围均为*m*/*z* 200～1 000, 归一化碰撞能量 (Normalized Collision Energy, NCE) 为30、50和70 eV。

质量控制 采用质控样品 (quality control, QC) 检测系统的稳定性[32]。QC样品是由匀浆后的样品各取100 μL混合得到。在对样品进行分析前, 为平衡系统先运行5次QC样品。在样品的检测过程中, 每检测5个正常样品后运行1次QC样品, 以衡量系统的稳定性。

数据处理 采用MS convert进行数据转换, 质谱分析原始谱图的数据转换为R语言 (R Project V3.2.2, The University of Auckland, New Zealand) 可识别的格式后, 进行峰匹配、峰对齐、峰提取和归一化处理, 然后使用Simca-P软件 (V13.0, MKS Data Analytics Solutions, Umea, Sweden) 进行主成分分析 (principal component analysis, PCA), 观察各组分分离趋势[33]。为获取更加可靠的代谢物的组间差异与实验组的相关程度信息, 采用偏最小二乘法-判别分析 (partial least squares-discriminant analysis, PLS-DA) 的统计方法对结果进行分析。通过置换检验 (permutation test), 对模型有效性做进一步的检验[34]。PLS-DA模型第一主成分的变量投影重要度 (variable importance in the projection, VIP) 大于1的标准筛选差异性代谢物。同时, 使用Mass Profiler Professional (V12.6.1, 美国Agilent Technologies) 软件对SHR组与正常组数据进行*t*检验(Student's *t*-test), 保留*P*值小于0.05的变量, 筛选差异倍数 (fold change) 大于等于2, 作为潜在生物标记物。同时并通过人类代谢组数据库 (the human metabolome database, HMDB), 京都基因与基因组百科全书 (Kyoto encyclopedia of genes and genomes, KEGG)[35]和脂质图谱数据库 (lipid maps databases), 寻找差异代谢物和映射的代谢通路。

结果

1 钩藤乙醇提取物对自发性高血压大鼠的血压调节作用

通过无创血压仪在尾动脉上测量 (给药前和给药四周后) 的收缩压 (systolic blood pressure, SBP)。血压数据$\bar{x}$ ± SD表示, 通过SPSS 17.0软件进行单因素方差分析。从图1中可以看出, 治疗前, 治疗组和SHR组血压均高于正常组, 表明SHR血压均明显高于正常组大鼠, 在使用钩藤治疗4周后, 治疗组血压明显下降 (*P*< 0.05)。钩藤治疗后血压降低, 且随着给药时间的延长, 血压下降越明显。说明钩藤可以降低自发性高血压大鼠的血压, 对高血压大鼠有一定的治疗作用 (图1)。

2 UPLC-Q-Exactive Orbitrap MS稳定性评价

QC样本实验数据导入Simca-P软件, QC数据间

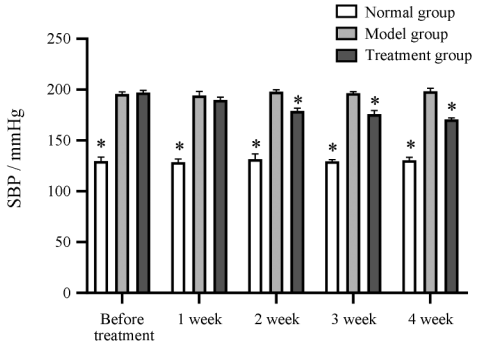

Figure 1 Blood pressure changes of spontaneously hypertension rats (SHR) after 4 weeks of continuous administration. $^{*}P$<0.05 *vs* model group. SBP: Systolic blood pressure

聚类紧密, 并集中分布于95%可信区间内, 表明数据质量可靠。为进一步验证数据质量的可靠性, 从QC样本中选取质量数从低到高的10个离子, 离子信号用*m/z*与t_R (min)表示, 计算各离子相应强度的RSD值<5% (表1), 说明数据可靠。

Table 1 Relative standard deviation (RSD) values of 10 ion signals in positive and negative ion modes

Positive mode (*m/z*)	t_R /min	RSD (%, *n*=9)	Negative mode (*m/z*)	t_R /min	RSD (%, *n*=9)
437.344 73	9.45	4.13	300.263 68	7.93	2.67
505.308 86	8.57	3.13	350.127 24	3.04	7.04
585.312 27	9.47	4.73	400.187 19	9.71	1.55
613.442 97	9.25	4.57	426.924 11	15.67	4.20
667.525 89	13.50	2.88	470.279 72	9.70	2.30
685.498 81	13.44	2.74	508.340 74	8.48	1.35
746.558 88	12.01	2.53	550.292 13	8.58	0.62
790.621 11	12.88	2.53	606.273 35	5.71	3.21
818.571 22	11.58	2.09	763.511 32	11.00	0.74
950.593 13	10.74	3.38	910.507 95	10.66	2.20

3 差异性标志物筛选和质谱解析

正、负离子模式下, PCA结果显示正常组与SHR组样本呈现出分离趋势, 无交叉与重叠。100次排列置换检验结果显示: R^2<0.5, Q^2<0模型拟合较好[36], 无过拟合现象。结果见图2。

4 差异性标志物质谱鉴定

参考相关的文献[37,38], 利用Xcalibur软件推测分子式, 然后根据其碎片离子信息推测该化合物的断裂规律和结构类型。最后, 结合常见代谢物的保留时间和代谢物数据库检索, 检测代谢物的结构, 最终在肝组织中筛选出45个有差异的脂质代谢物, 见表2。根据化合物母离子信息初步筛选标志物后, 可以根据子离子信息分析脂质化合物的裂解规律, 提高脂质成分鉴定的准确性。

磷脂类成分, 以PG_1为例, 在电喷雾负离子模式测得分子离子峰为$[PG_1-H]^-$, 其二级碎片离子多为由酯键断裂而来的$[lysoPG_1-H]^-$或$[lysoPG_2-H]^-$, 而溶血磷脂类成分其二级碎片离子会产生脂肪链$[FA-H]^-$, 在电喷雾负离子模式中磷脂类成分通常会产生$[M+H]^+$。如图3所示, lysoPE (0∶0/20∶4)分子离子峰*m/z*为501.593 10。图3A和图3B所示, 主要碎片离子峰*m/z* 483.249 18为中性丢失($[lysoPE-H_2O+H]^+$), 303.233 49为($[FA-H]^-$), 502.329 44为($[lysoPE+H]^+$), 500.279 82 ($[lysoPE-H]^-$)。PE (22∶4/22∶5)分子离子峰*m/z*为841.562 15, 见图3C, 840.576 6为($[PE-H]^-$), 主要碎片离子峰*m/z* 329.269 96, 331.264 74为($[FA-H]^-$)。PG

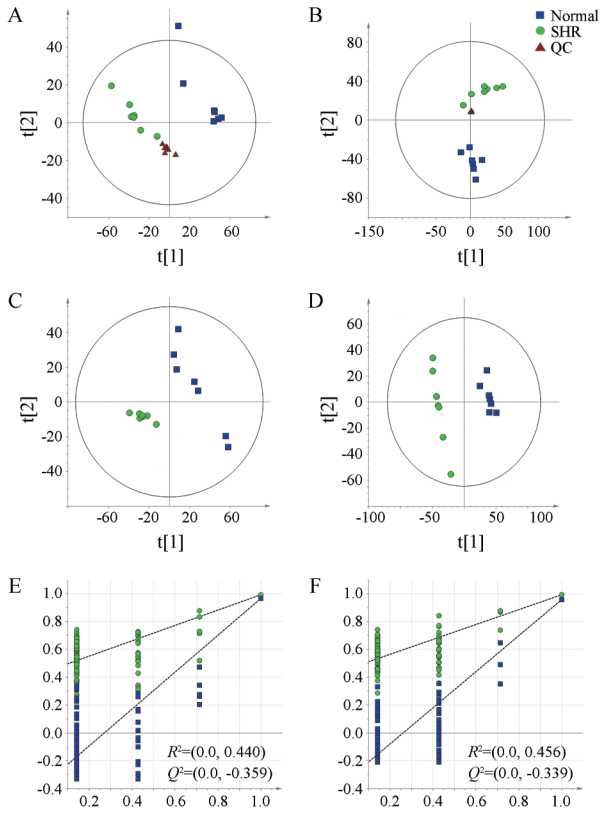

Figure 2 Principal component analysis (PCA) scores plots in positive (A) and negative (B) mode, partial least squares-discriminant analysis (PLS-DA) scores plots in positive (C) and negative (D) mode and permutation test in positive (E) and negative (F) mode. QC: Quality control; SHR: Spontaneously hypertensive rats. *n* = 7

(16∶0/18∶1)分子离子峰*m/z*为769.502 99 ($[M-H]^-$)的PG为例 (图3D), 主要碎片离子峰*m/z*为502.269 56 ($[lysoPG_1-H]^-$)、468.281 83 ($[lysoPG_2-H]^-$)、303.233 22 ($[FA_1-H]^-$)。

5 生物标志物分析

为进一步比较钩藤对生物标志物的干预作用, 比较了12种生物标志物的峰面积。使用SPSS 17.0进行单因素方差检验, 说明这些标志物的变化有显著性差异, 如图4所示。

通过对大鼠肝组织进行分析, 与正常组相比, SHR肝脏中Cer、亚油酸 (linoleic acid)、花生四烯酸 (arachidonic acid)、溶血磷脂酰胆碱 (lysophosphatidylcholine, lysoPC)、TAG的含量升高, 同时SM、PC、磷脂酸 (phosphatidic acid, PA)、甘油二酯 (diacylglycerol, DAG)的含量下降, 表明其代谢紊乱主要与鞘脂类代谢、脂肪酸代谢以及甘油磷脂代谢相关。经钩藤干预后不同程度地纠正了脂质代谢的异常, 说明钩藤对SHR肝脏脂质紊乱有一定的调节作用。

Table 2 Potential biomarkers of liver in SHR. ↑ and ↓ represent high and low level in SHR in comparison with normal group, separately. Product ion in positive ion mode is $[M-H_2O+H]^+$; product ion in negative mode is $[FA-H]^-$; PC: Phosphatidylcholine; lysoPC: Lysophosphatidylcholine; PE: Phosphatidyl ethanolamine; lysoPE: Lysophosphatidyl ethanolamine; PG: Phosphatidylglycerol; PS: Phosphatidylserine; PI: Phosphatidylinositol; SM: Sphingolipid; Cer: Ceramide; CE: Cholesteryl ester; DAG: Diacylglycerol; TAG: Triglyceride

Name	Trend (P<0.05 *vs* SHR)	t_R /min	*m/z* (measured)	*m/z* (true)	Deviation (10^{-6})	Product ion	Chemical formula	Class	Fragments
Stearoylgly cerophosphoinositol	↑	7.03	601.333 70	600.327 46	2.83		$C_{27}H_{53}O_{12}P$	Glycerophospholipids	$[M+H]^+$
3-Methyl-5-pentyl-2-furanundecanoic acid	↑	5.74	337.272 86	336.266 45	4.55		$C_{21}H_{36}O_3$	Fatty acids and conjugates	$[M+H]^+$
α-Linoleoylcholine	↑	6.59	367.339 42	366.337 20	15.61		$C_{23}H_{44}NO_2$	Organonitrogen compounds	$[M+H]^+$
CE (22∶4)	↑	15.72	699.628 50	700.615 83	29.42	331.265 08	$C_{49}H_{80}O_2$	Steroid esters	$[M-H]^-$
Galabiosylceramide (d18∶1/22∶0)	↑	16.41	946.696 36	946.341 40	24.55		$C_{52}H_{99}NO_{13}$	Sphingolipids	$[M+H]^+$
lysoPC (20∶0)	↑	9.22	552.401 80	551.395 08	2.21	534.425 35	$C_{28}H_{58}NO_7P$	Glycerophospholipids	$[M+H]^+$
lysoPE (0∶0/18∶2)	↓	5.75	476.278 89	477.285 53	2.72	305.239 81	$C_{23}H_{44}NO_7P$	Glycerophospholipids	$[M-H]^-$
lysoPE (0∶0/20∶3)	↓	5.71	502.284 08	503.301 19	18.22	305.239 78	$C_{25}H_{46}NO_7P$	Glycerophospholipids	$[M-H]^-$
lysoPE (0∶0/20∶4)	↓	5.71	500.279 10	501.285 53	3.01	303.233 40	$C_{25}H_{44}NO_7P$	Glycerophospholipids	$[M-H]^-$,
	↓		502.292 00	501.285 53	2.93	483.249 18			$[M+H]^+$
lysoPE (0∶0/22∶5)	↓	6.14	526.295 35	527.301 18	4.00	329.249 57	$C_{27}H_{46}NO_7P$	Glycerophospholipids	$[M-H]^-$,
	↓		528.307 80	527.301 18	2.50				$[M+H]^+$
PA (20∶4/2∶0)	↓	5.70	504.297 97	486.274 64	16.64	487.376 13 $[M+H]^+$	$C_{25}H_{43}O_7P$	Glycerophospholipids	$[M+H_2O+H]^+$
PC (22∶6/20∶0)	↓	12.67	862.630 20	861.624 75	2.89	844.643 37	$C_{50}H_{88}NO_8P$	Glycerophospholipids	$[M+H]^+$
PC (14∶0/18∶2)	↓	11.61	728.524 96	729.530 85	2.81		$C_{40}H_{76}NO_8P$	Glycerophospholipids	$[M-H]^-$
PC (14∶0/18∶4)	↓	10.85	724.493 70	725.499 55	2.88		$C_{40}H_{72}NO_8P$	Glycerophospholipids	$[M-H]^-$
PC (14∶0/20∶2)	↓	12.34	756.556 10	757.562 15	2.49	307.264 01	$C_{42}H_{80}NO_8P$	Glycerophospholipids	$[M-H]^-$
PC (20∶3/14∶0)	↓	11.53	756.544 70	755.546 50	12.89	307.264 01	$C_{42}H_{78}NO_8P$	Glycerophospholipids	$[M-H]^-$
PC (14∶0/20∶4)	↓	11.51	752.524 50	753.530 85	2.11	303.233 40	$C_{42}H_{76}NO_8P$	Glycerophospholipids	$[M-H]^-$,
	↓		754.531 60	753.530 85	9.54	736.498 47			$[M+H]^+$
PC (14∶1/22∶2)	↓	12.21	782.562 56	783.577 80	9.32	335.059 90	$C_{44}H_{82}NO_8P$	Glycerophospholipids	$[M-H]^-$
PC (18∶4/20∶5)	↓	10.54	798.531 00	799.515 20	29.69	301.217 53	$C_{46}H_{74}NO_8P$	Glycerophospholipids	$[M-H]^-$
PC (24∶0/15∶0)	↑	14.33	846.680 36	845.687 35	19.63	828.703 31	$C_{48}H_{96}NO_8P$	Glycerophospholipids	$[M+H]^+$
PE (14∶1/24∶1)	↓	12.77	770.572 14	771.577 80	2.95	364.961 61	$C_{43}H_{82}NO_8P$	Glycerophospholipids	$[M-H]^-$
PE (18∶2/24∶1)	↓	12.37	826.620 40	825.624 75	14.89	808.581 40	$C_{47}H_{88}NO_8P$	Glycerophospholipids	$[M+H]^+$
PE (18∶3/24∶1)	↓	12.37	824.614 20	823.609 10	3.45	806.567 32	$C_{47}H_{86}NO_8P$	Glycerophospholipids	$[M+H]^+$

Continued

Name	Trend (P<0.05 *vs* SHR)	t_R /min	m/z (measured)	m/z (true)	Deviation (10^{-6})	Product ion	Chemical formula	Class	Fragments
PE (18∶4/24∶1)	↓	11.58	822.596 07	821.593 45	6.48	804.550 11	$C_{47}H_{84}NO_8P$	Glycerophospholipids	$[M+H]^+$
PE (20∶1/20∶3)	↓	11.58	796.583 20	795.577 80	6.48	778.562 93	$C_{45}H_{82}NO_8P$	Glycerophospholipids	$[M+H]^+$
PE (20∶3/22∶5)	↑	12.62	814.554 90	815.546 50	3.19	329.270 17	$C_{47}H_{78}NO_8P$	Glycerophospholipids	$[M-H]^-$
PE (22∶1/22∶6)	↓	12.59	844.608 70	845.593 45	20.04	327.233 43 337.145 39	$C_{49}H_{84}NO_8P$	Glycerophospholipids	$[M-H]^-$
PE (22∶2/22∶6)	↓	11.58	842.583 40	843.577 80	27.42	327.233 25 335.052 28	$C_{49}H_{82}NO_8P$	Glycerophospholipids	$[M-H]^-$
PE (22∶4/22∶5)	↓	11.58	840.576 60	841.562 15	16.05	329.249 15 331.264 77	$C_{49}H_{80}NO_8P$	Glycerophospholipids	$[M-H]^-$
PG (16∶0/20∶4)	↓	9.80	769.503 60	770.509 78	26.61	303.233 34	$C_{42}H_{75}O_{10}P$	Glycerophospholipids	$[M-H]^-$
PGP (18∶0/22∶4)	↓	9.67	905.505 86	906.538 71	2.28	331.264 98	$C_{46}H_{84}O_{13}P_2$	Glycerophospholipids	$[M-H]^-$
PI (18∶0/20∶2)	↓	10.13	891.577 30	890.588 42	27.48		$C_{47}H_{87}O_{13}P$	Glycerophospholipids	$[M+H]^+$
PS (16∶0/22∶6)	↑	9.96	806.498 90	807.505 03	21.40	327.233 15	$C_{44}H_{74}NO_{10}P$	Glycerophospholipids	$[M-H]^-$
PS (20∶3/22∶6)	↑	10.46	856.512 10	857.520 68	2.24	305.249 33 327.233 31	$C_{48}H_{76}NO_{10}P$	Glycerophospholipids	$[M-H]^-$
PS (20∶3/22∶0)	↑	12.37	868.607 90	869.614 58	1.45	339.233 31 305.248 93	$C_{48}H_{89}NO_{13}$	Glycerophospholipids	$[M-H]^-$
DAG (22∶2/22∶6/0∶0)	↓	11.46	721.555 85	720.569 28	0.75		$C_{47}H_{76}O_5$	Glycerolipids	$[M+H]^+$
SM (d18∶1/22∶1)	↓	13.35	843.662 40	784.645 82	29.66	825.653 81	$C_{45}H_{89}N_2O_6P$	Sphingolipids	$[M+Hac-H]^+$
TAG (18∶4/20∶5/22∶6)	↑	16.41	945.694 30	944.689 39	29.80		$C_{63}H_{92}O_6$	Glycerolipids	$[M+H]^+$
TAG (20∶2n6/20∶3n6/18∶4)	↑	16.12	915.724 73	914.736 34	3.21		$C_{60}H_{98}O_6$	Glycerolipids	$[M+H]^+$
TAG (20∶5/16∶1/20∶5)	↑	16.86	897.692 60	896.689 39	21.37		$C_{59}H_{92}O_6$	Glycerolipids	$[M+H]^+$
TAG (22∶5/15∶0/22∶5)	↑	16.42	941.741 46	940.751 99	5.27		$C_{62}H_{100}O_6$	Glycerolipids	$[M+H]^+$
Cer (d18∶0/26∶0)	↑	14.15	678.605 96	679.684 25	29.94		$C_{44}H_{89}NO_3$	Sphingolipids	$[M-H]^-$
Linoleic acid	↑	7.67	301.218 80	280.240 23	16.71		$C_{18}H_{32}O_2$	Fatty acid	$[M+Na-2H]^{2-}$
Arachidonic acid	↑	5.74	337.272 86	304.240 23	24.03		$C_{20}H_{32}O_2$	Fatty acid	$[M+CH_3OH+H]^+$

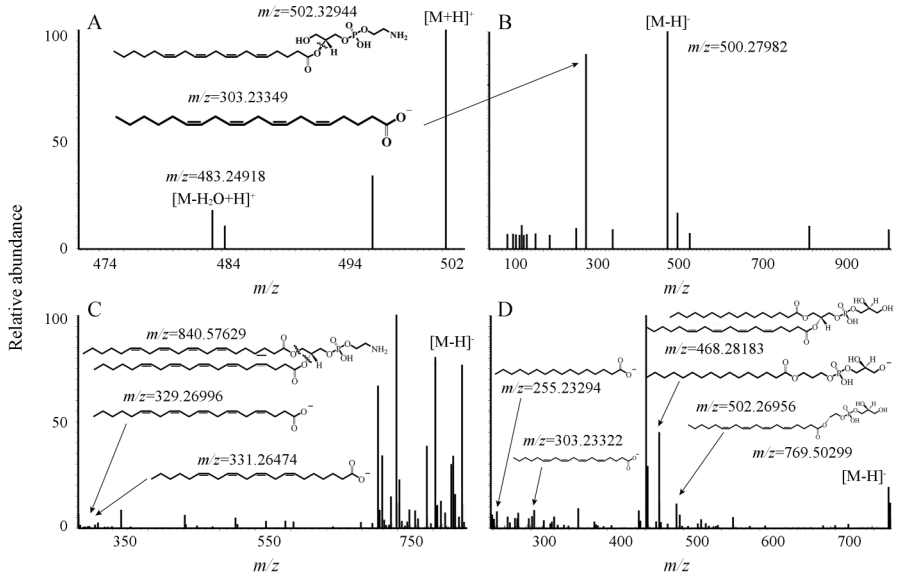

Figure 3　Mass spectrometry analysis of potential biomarkers. lysoPE (20∶4) *m/z* 502.329 44 positive ion mode (A), lysoPE (20∶4) *m/z* 500.279 82 negative ion mode (B), PE (22∶4/22∶5) *m/z* 840.576 29 negative ion mode (C), PG (16∶0/20∶4) *m/z* 769.502 99 negative ion mode (D)

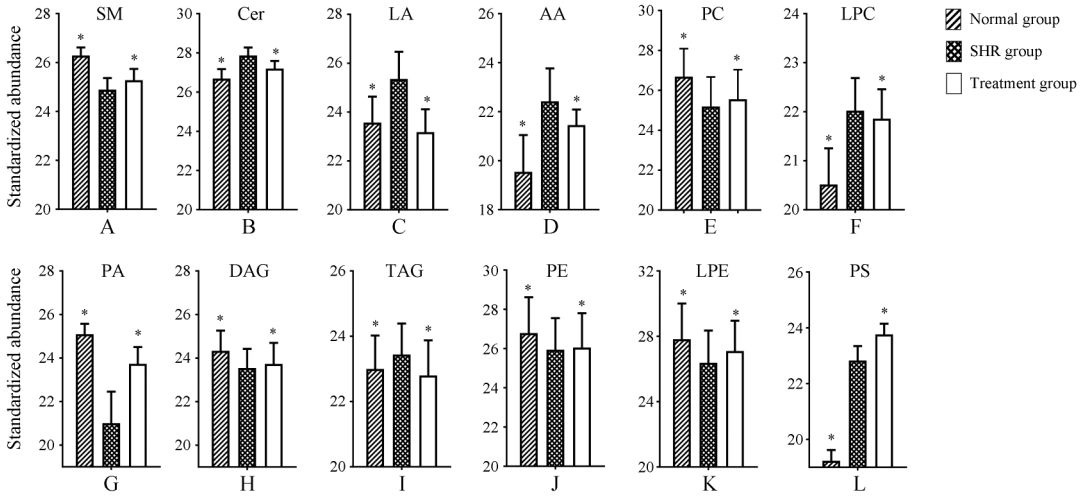

Figure 4　Relative peak areas of potential biomarkers in UHPLC-MS spectra of liver in SHR group in comparison with normal and treatment groups. $^{*}P<0.05$ *vs* SHR, $n = 7$, $\bar{x} \pm s$. LA: Linoleic acid; AA: Arachidonic acid; PA: Phosphatidic acid

讨论

肾素−血管紧张素−醛固酮系统 (renin-angiotensin-aldosterone system, RAAS) 中血管紧张素 II 激活鞘磷脂酶导致神经酰胺产生和释放[39,40]。本文研究表明 SHR 肝脏中鞘脂类成分代谢紊乱, 其中 Ceramide (Cer) 的升高是高血压产生的重要标志。

TAG 代谢产生的 FFA 破坏血管内皮细胞的完整性, 并升高 Ca^{2+} 离子通过性而导致平滑肌收缩增强, 促进高血压的发生发展[41-43]。Kulkarni 等[23]指出 DAG (16∶0/22∶5)、DAG (16∶0/22∶6) 和 PE (40∶6) 与遗传性高血压具有密切的关系。本研究发现高血压大鼠 DAG (22∶2/22∶6) 的含量比正常组低。Hu 等[24]研究发现, 高血压患者血浆的 TAG (48∶0, 48∶1, 48∶2, 48∶3, 50∶0, 50∶1, 50∶2, 50∶3, 50∶4, 50∶5, 52∶1, 52∶2, 52∶3, 52∶4, 52∶5, 52∶6, 54∶2, 54∶3, 54∶4, 54∶5, 54∶6, 56∶5, 56∶6, 56∶7, 56∶8, 56∶9) 等, 均表现为升高的趋势。本文发现的 TAG (59∶10, 56∶11, 60∶15) 在高血压组中的含量都比正常组高。本文研究发现 SHR 组的 DAG 与正常组相比明显下调, TAG 上调, 说明高血压与 TAG 在肝脏中的蓄积有关。同时作者发现 SHR 组 DAG 含量的下调与 PA 的减少有关。钩藤调节了高血压大鼠 DAG 和 TAG 代谢的过程。

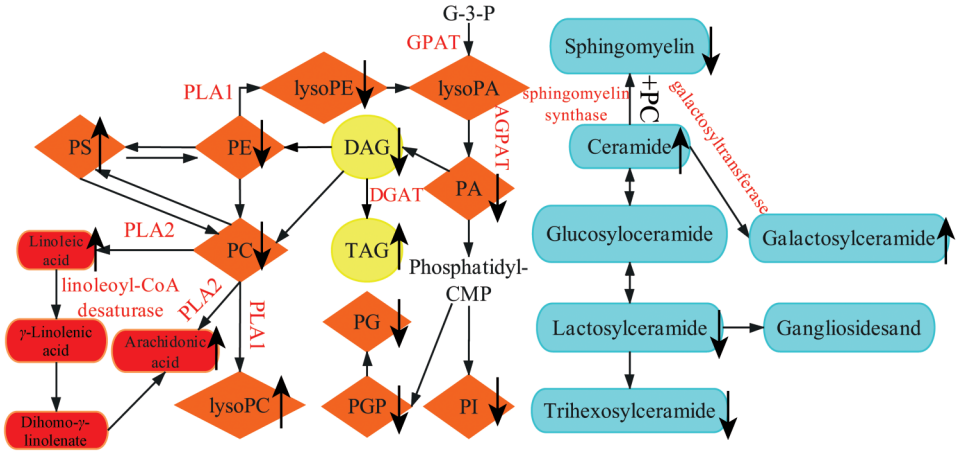

Figure 5 The metabolic network of liver endogenous metabolites. ↑ and ↓ represent high and low level in SHR in comparison with normal group, separately. Phosphate metabolic pathway (orange), glyceride metabolic pathway (yellow), sphingolipid metabolic pathway (blue), arachidonic acid metabolic pathway (red). PG: Phosphatidylglycerol; PI: Phosphatidylinositol; PGP: Glycerophospholipid; G-3-P: Glycerol-3-phosphate; PLA_1: Phospholipase A_1; PLA_2: Phospholipase A_2; DGAT: Diacylglycerol *O*-acyltransferase; GPAT: Glycerol-3-phosphateacyl-transferase; AGPAT: Acylglycerol-3-phosphateacyl-transferase

同时, 肝脏中 TAG 的增多与 PC 的减少有关。PC 在肝脏中可以促进肝脏中 TAG 的代谢, 减少 TAG 在肝脏中的沉积。同时, PC 的乳化特性可以减少甘油三酯和胆固醇在血管壁上的沉积[44], 从而达到调节脂质紊乱。Kulkarni 等[23]认为不同亚型的 PC 中, PC (34∶4) 的减少是引起脂质代谢紊乱的重要原因。而本研究发现 SHR 与正常组相比所有亚型的 PC 都呈现下降的趋势。

综上, 本文通过研究, 发现了自发性高血压大鼠肝脏脂质代谢紊乱。本实验通过数据统计和分析后, 查找出了 44 种显著差异性代谢物和 4 个代谢通路 (图 5)。本实验通过自发性高血压大鼠实验初步猜测, 高血压引起了脂质代谢紊乱, 钩藤治疗后, 脂质和脂肪酸的含量回调。脂质和脂肪酸的含量回调说明高血压存在脂质代谢紊乱, 并进一步加重其发展, 钩藤调控肝脏脂质代谢进而发挥降血压作用。

References

[1] Nikolic SB, Sharman JE, Adams MJ, et al. Metabolomics in hypertension [J]. J Hypertens, 2014, 32: 1159-1169.

[2] He J, Gu D, Chen J, et al. Premature deaths attributable to blood pressure in China: a prospective cohort study [J]. Lancet, 2009, 374: 1765-1772.

[3] Zhu ZM, Wang HJ, Yu RX, et al. Lipidomics analysis of liver in hypertension with syndrome of upper hyperactivity of liver yang rats [J]. Chin J Tradit Chin Med Pharm (中华中医药杂志), 2018, 33: 5361-5365.

[4] Hinterwirth H, Stegemann C, Mayr M. Lipidomics: Quest for Molecular Lipid Biomarkers in Cardiovascular Disease [J]. Circ Cardiovasc Genet, 2014, 7: 941-954.

[5] Farwanah H, Kolter T. Lipidomics of glycosphingolipids [J]. Metabolites, 2012, 2: 134-164.

[6] Eshigina S, Gapparov MM, Mal'Tsev GI, et al. Influence of dietary therapy containing sunflower oil fortified with phospholipids on the lipid metabolism in patients with hypertension and obesity [J]. Vopr Pitan, 2007, 76: 58-62.

[7] Arnold C, Markovic M, Blossey K, et al. Arachidonic acid-metabolizing cytochrome P450 enzymes are targets of ω-3 fatty acids [J]. J Biol Chem, 2010, 285: 32720-32733.

[8] Zheng W, Kollmeyer J, Symolon H, et al. Ceramides and other bioactive sphingolipid backbones in health and disease: lipidomic analysis, metabolism and roles in membrane structure, dynamics, signaling and autophagy [J]. Biochim Biophys Acta Biomembr, 2006, 1758: 1864-1884.

[9] Law SH, Chan ML, Marathe GK, et al. An updated review of lysophosphatidylcholine metabolism in human diseases [J]. Int J Mol Sci, 2019, 20: 1149-1173.

[10] Zhu Y, Liu H, Zhang M, et al. Fatty liver diseases, bile acids, and FXR [J]. Acta Pharm Sin B, 2016, 6: 409-412.

[11] Kwong E, Li Y, Hylemon PB, et al. Bile acids and sphingosine-1-phosphate receptor 2 in hepatic lipid metabolism [J]. Acta Pharm Sin B, 2015, 5: 151-157.

[12] Chen H, Chen L, Liu D, et al. Combined clinical phenotype and lipidomic analysis reveals the impact of chronic kidney disease on lipid metabolism [J]. J Proteome Res, 2017, 16: 1566-1578.

[13] Walther A, Cannistraci CV, Simons K, et al. Lipidomics in major depressive disorder: a systematic review [J]. Front Psychiatry, 2018, 9: 459-470.

[14] Nam M, Choi MS, Jung S, et al. Lipidomic profiling of liver tissue from obesity-prone and obesity-resistant mice fed a high

fat diet [J]. Sci Rep, 2015, 5: 16984.

[15] Nguyen P, Leray V, Diez M, et al. Liver lipid metabolism [J]. J Anim Physiol Anim Nutr (Berl), 2008, 92: 272-283.

[16] Graessler J, Schwudke D, Schwarz PE, et al. Top-down lipidomics reveals ether lipid deficiency in blood plasma of hypertensive patients [J]. PLoS One, 2009, 4: e6261.

[17] Xie J, Jiang HQ, Li YL, et al. Study on the intervention effects of Pinggan prescription on spontaneously hypertensive rats based on metabonomic and pharmacodynamic methods [J]. Chin J Integr Med, 2019, 25: 348-353.

[18] Donovan EL, Pettine SM, Hickey MS, et al. Lipidomic analysis of human plasma reveals ether-linked lipids that are elevated in morbidly obese humans compared to lean [J]. Diabetol Metab Syndr, 2013, 5: 24-37.

[19] Miao QY, Gao W, Li J, et al. Progress on lipidomics analytical methods and their applications in studies of traditional Chinese medicines [J]. China J Chin Mater Med (中国中药杂志), 2019, 44: 1760-1766.

[20] Han X, Gross RW. Global analyses of cellular lipidomes directly from crude extracts of biological samples by ESI mass spectrometry: a bridge to lipidomics [J]. J Lipid Res, 2010, 24: 1071-1079.

[21] Yang K, Han X. Lipidomics: techniques, applications, and outcomes related to biomedical sciences [J]. Trends Biochem Sci, 2016, 41: 954-969.

[22] Han XL. Lipidomics for studying metabolism [J]. Nat Rev Endocrinol, 2016, 12: 668-679.

[23] Kulkarni H, Meikle PJ, Mamtani M, et al. Plasma lipidomic profile signature of hypertension in Mexican American families: specific role of diacylglycerols [J]. Hypertension, 2013, 62: 453-454.

[24] Hu C, Kong H, Qu F, et al. Application of plasma lipidomics in studying the response of patients with essential hypertension to antihypertensive drug therapy [J]. Mol Biosyst. 2011, 7: 3271-3279.

[25] Ho SC, Ho YF, Lai TH, et al. Traditional Chinese herbs against hypertension enhance memory acquisition [J]. Am J Chin Med, 2012, 33: 787-795.

[26] Heitzman ME, Neto CC, Winiarz E, et al. Ethnobotany, phytochemistry and pharmacology of *Uncaria* (Rubiaceae) [J]. Phytochemistry, 2005, 66: 5-29.

[27] Sakakibara I, Terabayashi S, Kubo M, et al. Effect on locomotion of indole alkaloids from the hooks of *Uncaria* plants [J]. Phytomed, 1999, 6: 163-168.

[28] Zhang F, Sun AS, Yu LM, et al. Effects of isorhynchophylline on angiotensin II-induced proliferation in rat vascular smooth muscle cells [J]. J Pharm Pharmacol, 2009, 60: 1673-1678.

[29] Tian YP, Jiang F, Li YL, et al. Evaluation of the anti-hypertensive effect of Tengfu Jiangya tablet by combination of UPLC-Q-exactive-MS-based metabolomics and iTRAQ-based proteomics technology [J]. Biomed Pharmacother, 2018, 100: 324-334.

[30] Yang WQ, Li YL, Xie J, et al. Exploratory study of quantification diagnostic standard on common traditional Chinese medicine syndromes of hypertension [J]. Chin J Tradit Chin Med Pharm (中华中医药杂志), 2016, 31: 2008-2012.

[31] Matyash V, Liebisch G, Kurzchalia TV, et al. Lipid extraction by methyl-tert-butyl ether for high-throughput lipidomics [J]. J Lipid Res, 2008, 49: 1137-1146.

[32] Wilson ID, Gika H, Theodoridis G, et al. Global metabolic profiling procedures for urine using UPLC-MS [J]. Nat Protoc, 2010, 5: 1005-1018.

[33] A JY, He J, Sun RS. Multivariate statistical analysis for metabolomic data: the key points in principal component analysis [J]. Acta Pharm Sin (药学学报), 2018, 53: 929-937.

[34] Zhang JX, Sun L, Pang J, et al. Non-targeted metabolomics in septic mice infected with *Klebsiella pneumoniae* [J]. Acta Pharm Sin (药学学报), 2018, 53: 1122-1130.

[35] Wang DF, Wang YL, Wang YW, et al. Effect of Huangqin Tang on serum metabolic profile in rats with ulcerative colitis based on UHPLC-MS [J]. Acta Pharm Sin (药学学报), 2017, 52: 108-114.

[36] Song J, Pang YY, Gao L, et al. Effects of *Scutellaria baicalensis* Georgi flowers on *D*-galactose induced aging in rats based on serum metabolomics [J]. Acta Pharm Sin (药学学报), 2019, 54: 533-539.

[37] Byeon SK, Lee JY, Moon MH. Optimized extraction of phospholipids and lysophospholipids for nanoflow liquid chromatography-electrospray ionization-tandem mass spectrometry [J]. Analyst, 2011, 137: 451-458.

[38] Stübiger G, Pittenauer E, Allmaier G. MALDI seamless post-source decay fragment ion analysis of sodiated and lithiated phospholipids [J]. Anal Chem, 2008, 80: 1664-1678.

[39] Borodzicz S, Czarzasta K, Kuch M, et al. Sphingolipids in cardiovascular diseases and metabolic disorders [J]. Lipids Health Dis, 2015, 14: 55-63.

[40] Berry C. Angiotensin receptors: signaling, vascular pathophysiology, and interactions with ceramide [J]. Am J Physiol Heart Circ Physiol, 2001, 281: H2337-H2365.

[41] Kalepu S, Manthina M, Padavala V. Oral lipid-based drug delivery systems-an overview [J]. Acta Pharm Sin B, 2013, 3: 361-372.

[42] Lundman P, Eriksson M, Schenckgustafsson K, et al. Transient triglyceridemia decreases vascular reactivity in young, healthy men without risk factors for coronary heart disease [J]. Circulation, 1997, 96: 3266-3268.

[43] Cahova M, Chrastina P, Hansikova H, et al. Carnitine supplementation alleviates lipid metabolism derangements and protects against oxidative stress in non-obese hereditary hypertriglyceridemic rats [J]. Appl Physiol Nutr Metab, 2015, 40: 280-291.

[44] Mari M, Fernandez-Checa JC. Sphingolipid signalling and liver diseases [J]. Liver Int, 2007, 27: 440-450.